Chinese Journal of Chemical Engineering 37 (2021) 217–221

Contents lists available at ScienceDirect

Chinese Journal of Chemical Engineering

journal homepage: www.elsevier.com/locate/CJChE

Full Length Article

Ultrafine tuning of the pore size in zeolite A for efficient propyne removal from propylene

Chaohui He [1], Rajamani Krishna [2], Yang Chen [1], Jiangfeng Yang [1], Jinping Li [1], Libo Li [1,3,*]

[1] College of Chemistry and Chemical Engineering, Shanxi Key Laboratory of Gas Energy Efficient and Clean Utilization, Taiyuan University of Technology, Taiyuan 030024, China
[2] Van't Hoff Institute for Molecular Sciences, University of Amsterdam, Science Park 904, 1098 XH Amsterdam, the Netherlands
[3] Key Laboratory of Coal Science and Technology, Taiyuan University of Technology, Taiyuan 030024, China

ARTICLE INFO

Article history:
Received 29 September 2020
Received in revised form 3 November 2020
Accepted 13 November 2020
Available online 22 January 2021

Keywords:
Type-A zeolite
Ion-exchange
Pore tuning
Propyne/propylene separation
Breakthrough experiments

ABSTRACT

The removal of trace propyne (C_3H_4) from propyne/propylene (C_3H_4/C_3H_6) mixtures is a technical and challenging task during the production of polymer-grade propylene in view of their very similar size and physical properties. While some progress has been made, it is still very challenging to use some highly stable and commercially available porous materials via an energy-efficient adsorptive separation process. Herein, we report the ultrafine tuning of the pore apertures in type-A zeolites for the highly efficient removal of trace amounts of C_3H_4 from C_3H_4/C_3H_6 mixtures. The resulting ion-exchanged zeolite 5A exhibits a large C_3H_4 adsorption capacity (2.3 mmol g^{-1} under 10^{-4} MPa) and high C_3H_4/C_3H_6 selectivity at room temperature, which were mainly attributed to the ultrafine-tuned pore size that selectively blocks C_3H_6 molecules, while maintaining the strong adsorption of C_3H_4 at low pressure region. High purity of C_3H_6 (>99.9999%) can be directly obtained on this material under ambient conditions, as demonstrated by the experimental breakthrough curves obtained for both 1/99 and 0.1/99.9 (*V*/*V*) C_3H_4/C_3H_6 mixtures.

1. Introduction

Propylene (C_3H_6) is a key olefin raw material used for petrochemical production, second in importance to ethylene [1]. During the production of C_3H_6, trace amounts of propyne (C_3H_4) (0.1% or 1%) is inevitably generated as an impurity and is highly undesirable. To meet the criterion of polymer-grade C_3H_6, trace amounts of the C_3H_4 impurity must be removed to be <0.0005% or even 0.0001%. However, these two molecules have very close structural dimensions (C_3H_4: 0.416 nm × 0.401 nm × 0.651 nm and C_3H_6: 0.416 nm × 0.465 nm × 0.644 nm) and similar physical properties, which makes the removal of C_3H_4 from C_3H_6 highly challenging [2,3].

Traditional cryogenic distillation and catalytic hydrogenation technologies [4] used to purify C_3H_6 usually suffer from some obvious drawbacks, such as high energy consumption, low efficiency and secondary pollution. Finding an alternative method will reduce the energy needed to make the 120 million tons of propylene manufactured worldwide each year. Adsorptive separation based on porous materials is more energy-efficient [5–15]. In 2017, we reported the first example of a porous material (ELM-12) used for the efficient removal of C_3H_4 from a C_3H_4/C_3H_6 mixture *via* an adsorptive separation method [16]. Subsequently, many microporous metal–organic frameworks (MOFs), such as SIFSIX-3-Ni, ZJUT-1, ZU-62, NKMOF-Ni-1 (SIFSIX = SiF_6^{2-}), have been developed as highly selective C_3H_4 adsorbents for the highly selective capture of C_3H_4 from C_3H_6 [17–20]. However, these MOF materials have some drawbacks, including the high energy cost of regeneration due to strong C_3H_4 binding interactions and low structural stability upon exposure to moisture and/or sulfur compounds, especially in the presence of open metal sites that can lead to oligomerization of the olefins and ultimately block their porous channels. Therefore, it is highly urgent to develop stable and commercially available adsorbents with high C_3H_4/C_3H_6 adsorption selectivity, excellent gas mixture separation performance and structural stability.

Small pore zeolites have attracted a lot of attention for gas separation/purification in recent years [21–23]. Due to their porous channels, some zeolite exhibit high selectivity for some gas mixtures, including CO_2/CH_4, CH_4/N_2, ethane/ethylene and propane/

* Corresponding author at: College of Chemistry and Chemical Engineering, Shanxi Key Laboratory of Gas Energy Efficient and Clean Utilization, Taiyuan University of Technology, Taiyuan 030024, China.
E-mail address: lilibo908@hotmail.com (L. Li).

https://doi.org/10.1016/j.cjche.2020.11.037

propylene [24–36]. However, with the exceptionally high purity requirement (C_3H_4 < 0.0001%) and small molecular difference between C_3H_4 and C_3H_6 (kinetic diameters: C_3H_4, ~0.42 nm; C_3H_6, ~0.46 nm), the efficient removal of C_3H_4 has been rarely reported using zeolites to date. At present, there is only one reported zeolite that can realize the separation of an equimolar C_3H_4/C_3H_6 mixture by confining isolated open Ni sites in an FAU zeolite [37]. However, molecular sieving and separation have not been realized because it is quite challenging to design ideal porous materials on traditional zeolites by fine-tuning the pore aperture size in 0.02–0.1 nm increments. Using an ion-exchange method to maximize the sieving effect for gas separation, it is possible to control the pore channels of traditional zeolites, thus allowing the entrance of C_3H_4, but hindering the diffusion of C_3H_6 to significantly increasing the separation performance [38–40].

Herein, we report the highly efficient separation of trace amounts of C_3H_4 from C_3H_6 using Na-exchanged zeolite 5A. This zeolite material has a suitable and robust pore size that can efficiently capture C_3H_4 molecules, while blocking C_3H_6 at low pressure, and thus exhibit high C_3H_4/C_3H_6 adsorption selectivity. In addition, trace amounts of C_3H_4 can be readily removed from a C_3H_4/C_3H_6 (1/99 and 0.1/99.9, *V*/*V*) mixture to produce high-purity propylene (>99.9999%) under ambient conditions.

2. Experimental

2.1. Synthesis of materials

NaA (Ca^{2+}), NaA and NaA (K^+) used in this study are powdered 5A, 4A, and 3A zeolite provided by Sigma-Aldrich. Ion-exchange was performed by exposing the as-received commercial zeolites to an excess of aqueous sodium chloride (NaCl, Sigma Aldrich) solution. 1 g of zeolite was treated with 50 ml of 1 mol·L^{-1} solution of NaCl for 2 h with stirring at 353 K. Afterwards, the exchanged material was washed thoroughly with distilled water, filtered and dried at 423 K. 5A (*x*Na^+), 5A (*y*Na^+), and 5A (*z*Na^+) in this work were converted from zeolite 5A *via* one, two, and three consecutive ion-exchange steps, respectively.

Propyne (C_3H_4, 99.99%), propylene (C_3H_6, 99.99%), helium (99.999%) and mixed gases comprised of C_3H_4/C_3H_6 (1/99 and 0.1/99.9, *V*/*V*) were purchased from Beijing Special Gas Co. Ltd, China.

2.2. Characterization

Powder X-ray diffraction (PXRD) was carried out on a BRUKER D8 ADVANCE diffractometer employing Cu K_α radiation operated at 30 kV over the 2θ range of 5°–40° at a scanning rate of 1 (°)·min^{-1}. Scanning electron microscopy (SEM) was performed using a Hitachi SU8010 scanning electron microscope.

2.3. Gas sorption measurements

An Intelligent Gravimetric Analyzer (IGA 001, Hiden, UK) was used to measure the C_3H_4 and C_3H_6 adsorption isotherms. The sorption isotherms of N_2 at 77 K and CO_2 at 273 K were measured on a Micromeritics ASAP 2020 analyzer. All the samples were activated at 473 K over 2 h to remove the guest molecules prior to actual measurement (see Fig. 1).

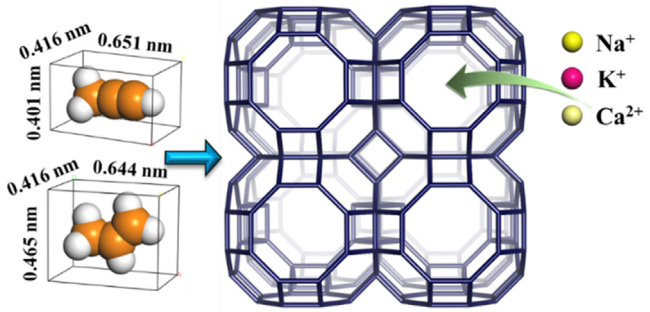

Fig. 1. A schematic of the fine-tuning of the pore size using ion-exchange in type-A zeolites for C_3H_4/C_3H_6 separation.

3. Results and Discussion

3.1. Characterization of ion-exchanged zeolite A

In view of the structure dimensions of C_3H_4 and C_3H_6, commercially available type-A zeolite with a similar pore size was selected to be used as a platform for C_3H_4/C_3H_6 separation (see Fig.1). Type-A zeolite can have different pore sizes from 0.3 to 0.5 nm *via* changing the cation (Na^+, Ca^{2+} and K^+) [41], whose gradual reduction in pore size of ~0.1 nm is not precise enough to differentiate the small size difference between C_3H_4 and C_3H_6. We speculated that there is still room for fine-tuning the pore size to further improve the C_3H_4/C_3H_6 separation performance. An appropriate pore size to maximize the sieving effect could be achieved by controlling the number of Na^+-exchange steps using 5A zeolite to precisely tailor the pore size with 0.01–0.02 nm increments and thus, improve the separation performance.

The pore size distributions of commercial and ion-exchanged type-A zeolite were first checked using N_2 sorption analysis at 77 K. Fig. 2 shows that when the cation was changed from Ca^{2+} to Na^+ and K^+, the pore size of the zeolite was reduced to block the entrance of N_2 at 77 K. For the Na^+-exchanged type-A zeolite (Fig. 2b), N_2 adsorption was decreased in smaller increments when compared to the commercial zeolite, which indicates that controlling the number of Na^+-exchange steps could precisely tailor the change in the pore size. In addition, all of the ion-exchanged zeolites maintained the main zeolite structure, as confirmed by PXRD analysis.

To further characterize the slight changes in the pore size during the ion-exchange process, the CO_2 adsorption isotherms were obtained at 273 K and used for our calculations. Fig. 3 shows the pore size of zeolite 5A varied from 0.52 to 0.44 nm with the number of ion-exchange steps, which were near to the kinetic diameter of C_3H_4 and C_3H_6, and may display a molecular sieving effect for gas mixture separation.

3.2. C_3H_6/C_3H_4 adsorption isotherms and selectivity of ion-exchanged zeolite A

In order to evaluate the effect of the changed pore size in zeolite A for the selective separation of C_3H_4 from C_3H_6, we conducted single-component sorption tests at 298 K. Fig. 4 shows the results obtained for commercial type-A zeolites (3A, 4A and 5A) with different micropore sizes to determine their basic adsorption properties for C_3H_4 and C_3H_6. The relevant adsorption uptakes of C_3H_4 and C_3H_6 sharply decreased with the pore size of commercial type-A zeolite, which indicates that C_3H_4 and C_3H_6 do not diffuse into the pore channels of NaA (zeolite 4A) and NaA (K^+) (zeolite 3A). However, the two C3 molecules can both be adsorbed in NaA (Ca^{2+}) because the adsorption isotherms of C_3H_4 and C_3H_6 were

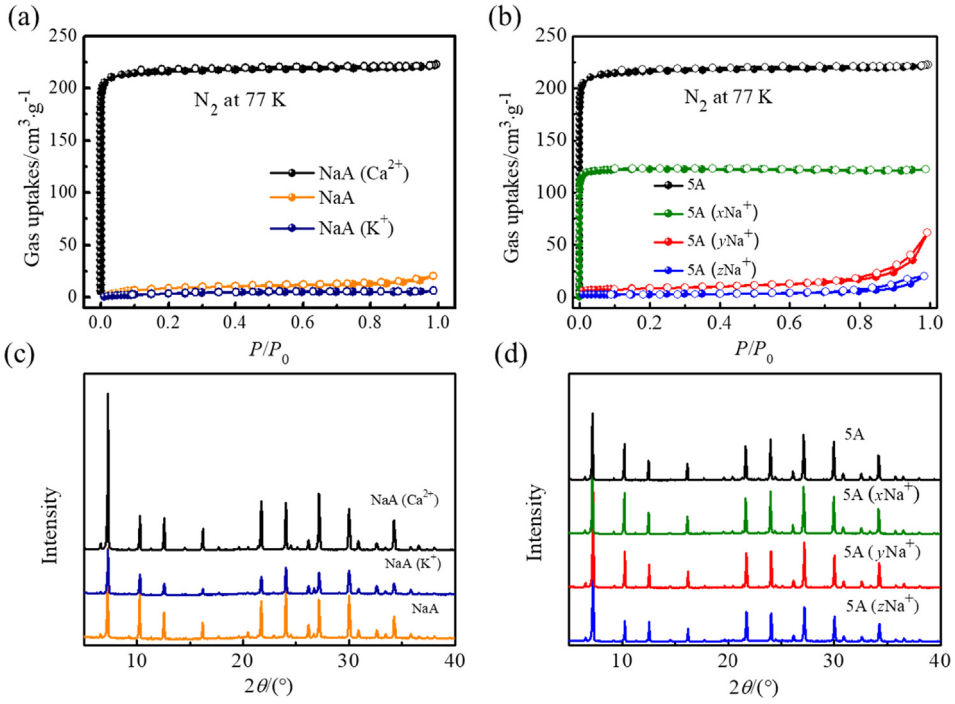

Fig. 2. N_2-sorption isotherms obtained for (a) NaA, NaA (Ca^{2+}) and NaA (K^+); (b) 5A, 5A (xNa$^+$), 5A (yNa$^+$), and 5A (zNa$^+$), and (c and d) their associated PXRD patterns.

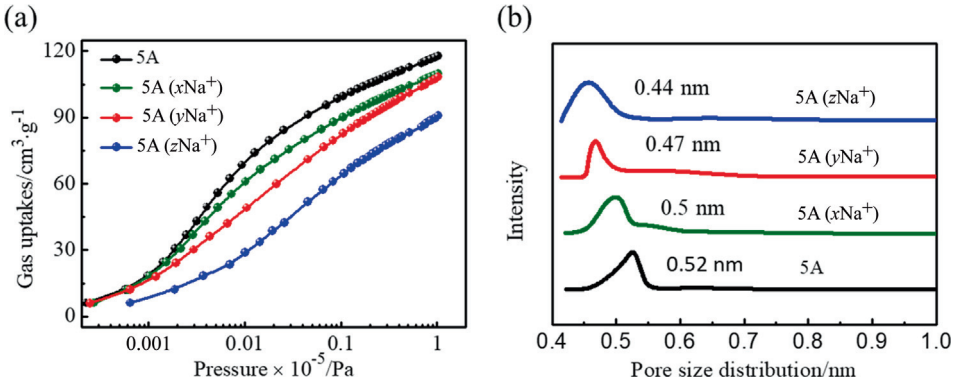

Fig. 3. (a) CO_2 adsorption isotherms obtained for the ion-exchanged NaA zeolites at 273 K and (b) their associated pore size distributions calculated using the D–R equation.

steep and quickly reached a near-saturated adsorption capacity at low pressure (C_3H_4 uptake reaches 2.3 mmol·g^{-1} under 10^{-4} MPa), indicating a possible platform for further optimization of the adsorption selectivity for C_3H_4/C_3H_6. Upon consecutive Na^+-exchange in zeolite 5A, the adsorption of C_3H_4 and C_3H_6 the observed for the different ion-exchanged zeolites gradually changes with the reduction in the pore size and 5A (yNa$^+$) exhibits the highest C_3H_4/C_3H_6 (1/99, V/V) selectivity (43), as calculated using the ideal adsorbed solution theory (IAST) method. This indicates our strategy to precisely tune the pore size to optimize the adsorption selectivity of C_3H_4/C_3H_6 is very effective. In addition, the pore size distribution further confirmed the relationship between the increase in the adsorption selectivity and pore size. 5A (yNa$^+$) with a pore size of 0.47 nm has the highest adsorption selectivity due to effectively blocking the adsorption of C_3H_6 at low pressure, while maintaining the strong adsorption for C_3H_4. When comparing the adsorption selectivity with typical MOFs (Fig. S2, in Supplementary Material), 5A (yNa$^+$) was larger than most of the previously reported MOFs (SIFSIX-2-Cu-i, UiO-66, MIL-100(Cr), Cu-BTC and ZIF-8), while lower than the benchmark MOFs (SIFSIX-3-Ni, ELM-12 and ZU-62). Given the thermal stability and production cost, 5A (yNa$^+$) has great advantage for industrial application. In addition, the heats of adsorption were calculated using the Virial equation to evaluate the binding affinity for C_3H_4 and C_3H_6 (Fig. S3). The heats of adsorption for zeolite 5A (yNa$^+$) toward C_3H_4 was 52 kJ·mol^{-1}, which was significantly larger than that toward C_3H_6 (30 kJ·mol^{-1}), which indicates the higher host–guest interactions between the framework and C_3H_4. Although the calculated heat of adsorption heat was slightly high, no hindrance was observed during the sorption process of C_3H_4 on zeolite 5A (yNa$^+$) and the adsorbent could easily be regenerated in vacuo or with a flow of helium under ambient conditions.

3.3. Breakthrough experiments

To further assess the separation performance of 5A (yNa$^+$) for actual C_3H_4/C_3H_6 mixtures (1/99 and 0.1/99.9 V/V), we conducted breakthrough experiments in a homemade apparatus. Fig. 5 shows 5A (yNa$^+$) displays an excellent separation performance for C_3H_4/C_3H_6 mixtures (1/99 and 0.1/99.9). C_3H_6 was quickly eluted from the column and reaches high purity, which can be stability maintained for a prolonged period of time until an C_3H_4 adsorption sat-

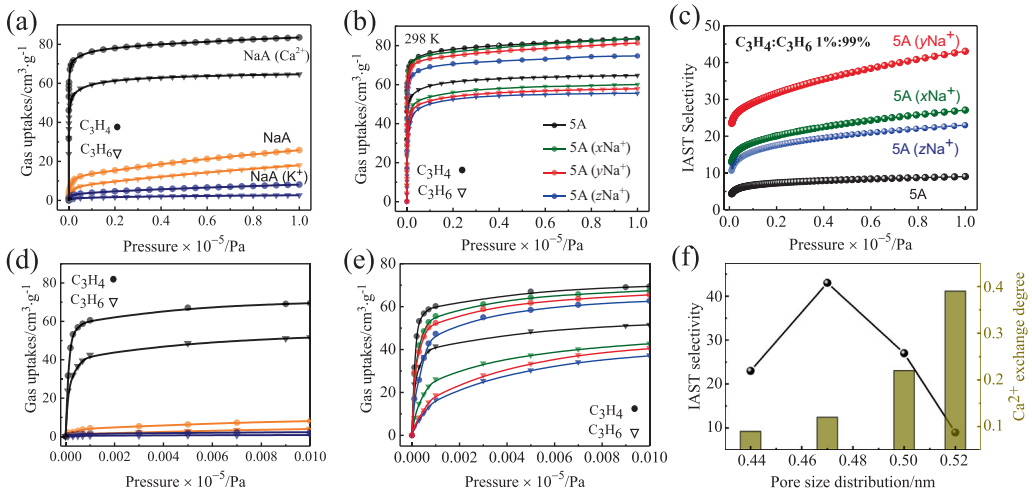

Fig. 4. C_3H_4 (circles) and C_3H_6 (triangles) adsorption isotherms obtained for the ion-exchanged NaA zeolites at 298 K in the region of (a and b) 0–0.1 MPa and (d and e) 0–0.001 MPa. (c) IAST selectivity of the ion-exchanged zeolites for C_3H_4/C_3H_6 (1/99, *V*/*V*) at 298 K. (f) A comparison of the IAST selectivity at 0.1 MPa, pore size distribution and degree of Ca-exchange in the zeolites.

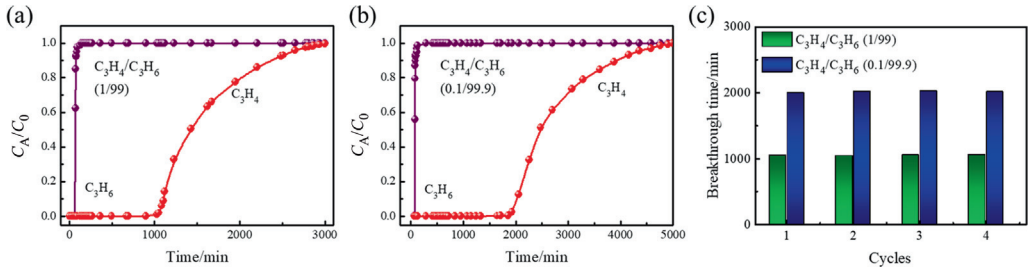

Fig. 5. (a and b) Experimental breakthrough curves obtained for 5A (yNa$^+$) using a C_3H_4/C_3H_6 mixture (1/99 and 0.1/99.9) at a gas velocity of 2.0 ml/min at 298 K and 0.1 MPa (C_3H_4, red; C_3H_6, purple). (c) The retained time of C_3H_6 obtained in the cycling tests of 5A (yNa$^+$) using 1/99 and 0.1/99.9 (*V*/*V*) C_3H_4/C_3H_6 mixtures.

uration is reached. The C_3H_4 breakthrough time for the C_3H_4/C_3H_6 mixtures (1/99 and 0.1/99.9 *V*/*V*) were 1000 and 1600 min, respectively. This great separation effect demonstrates that 5A (yNa$^+$) is suitable for this separation process and proved the precise fine-tuning of the pore size of zeolite A is an effective strategy to boost its separation performance. Furthermore, transient breakthrough simulations of the C_3H_4/C_3H_6 mixture (1/99, *V*/*V*) on 5A (yNa$^+$) at 298 K confirmed the actual separation results. High purity C_3H_6 can be recovered between 0–τ_{break} (2600 min) (Fig. S6). The breakthrough productivity of C_3H_6 calculated from the transient breakthrough curves of the C_3H_4/C_3H_6 mixture (1/99, *V*/*V*) was 71.7 mol·L^{-1} (Table S6), which was larger than most of the typical MOFs reported to date (SIFSIX-2-Cu-i and UiO-66). In addition, the cycle life and separation stability are also important for industrial applications. We carried out four cyclic breakthrough experiments for the separation of the C_3H_4/C_3H_6 mixtures (1/99 and 0.1/99.9, *V*/*V*) on 5A (yNa$^+$) at 298 K and the breakthrough times were almost unchanged, which indicates the separation performance can be largely maintained (Figs. S8–S9).

4. Conclusions

In summary, we have demonstrated that it is possible and feasible to prepare an efficient separation material for the separation of C_3H_4/C_3H_6 mixtures *via* ultrafine tuning of the pore size of zeolite A to selectively block C_3H_6, while retaining the high adsorption capacity for C_3H_4. The resulting Na-exchanged zeolite 5A exhibits both high selectivity and adsorption capacity for C_3H_4 and breakthrough experiments confirmed that this material can completely remove trace amounts of C_3H_4 from 1/99 and 0.1/99.9 (*V*/*V*) C_3H_4/C_3H_6 mixtures to afford a high C_3H_6 productivity and purity with a C_3H_4 concentration of <0.0001%. This work not only reveals a pathway for industrial C_3H_4/C_3H_6 separation, but also provides some guidance to facilitate the design of some practically useful materials at a reasonable cost for important hydrocarbon separation and purification processes in the near future.

Declaration of Competing Interest

The authors declare that they have no known competing financial interests or personal relationships that could have appeared to influence the work reported in this paper.

Acknowledgements

We acknowledge the financial support from the National Natural Science Foundation of China (21922810, 21908153, 21908155) and program of Innovative Talents of Higher Education Institutions of Shanxi. We are grateful for the supported by Cultivate Scientific Research Excellence Programs of Higher Education Institutions in Shanxi (CSREP).

Supplementary Material

Supplementary data to this article can be found online at https://doi.org/10.1016/j.cjche.2020.11.037.

References

[1] I. Amghizar, L.A. Vandewalle, K.M. Van Geem, G.B. Marin, New trends in olefin production, *Engineering* 3 (2017) 171–178.

[2] K. Adil, Y. Belmabkhout, R.S. Pillai, A. Cadiau, P.M. Bhatt, A.H. Assen, G. Maurin, M. Eddaoudi, Gas/vapour separation using ultra-microporous metal–organic frameworks: Insights into the structure/separation relationship, *Chem. Soc. Rev.* 46 (2017) 3402–3430.

[3] H. Li, L. Li, R.-B. Lin, W. Zhou, Z. Zhang, S. Xiang, B. Chen, Porous metal-organic frameworks for gas storage and separation: Status and challenges, *EnergyChem* 1 (2019) 100006.

[4] D. Teschner, J. Borsodi, A. Wootsch, Z. Révay, M. Hävecker, A. Knop-Gericke, S. D. Jackson, R. Schlögl, The roles of subsurface carbon and hydrogen in palladium-catalyzed alkyne hydrogenation, *Science* 320 (2008) 86–89.

[5] D.S. Sholl, R.P. Lively Seven chemical separations to change the world, *Nature* 532 (2016) 435–437.

[6] J.Y.S. Lin, Molecular sieves for gas separation, *Science* 353 (2016) 121–122.

[7] S. Chu, Y. Cui, N. Liu, The path towards sustainable energy, *Nat. Mater.* 16 (2017) 16–22.

[8] Y. Wang, S.B. Peh, D. Zhao, Alternatives to cryogenic distillation: Advanced porous materials in adsorptive light olefin/paraffin separations, *Small* 15 (2019) 1900058.

[9] L. Yang, S. Qian, X. Wang, X. Cui, B. Chen, H. Xing, Energy-efficient separation alternatives: Metal–organic frameworks and membranes for hydrocarbon separation, *Chem. Soc. Rev.* 49 (2020) 5359–5406.

[10] J.R. Li, R.J. Kuppler, H.C. Zhou, Selective gas adsorption and separation in metal-organic frameworks, *Chem. Soc. Rev.* 38 (2009) 1477–1504.

[11] L. Yang, W. Zhou, H. Li, A. Alsalme, L. Jia, J. Yang, J. Li, L. Li, B. Chen, Reversed ethane/ethylene adsorption in a metal–organic framework *via* introduction of oxygen, *Chin. J. Chem. Eng.* 28 (2020) 593–597.

[12] J. Ling, P. Xiao, A. Ntiamoah, D. Xu, P. Webley, Y. Zhai, Strategies for CO_2 capture from different CO_2 emission sources by vacuum swing adsorption technology, *Chin. J. Chem. Eng.* 24 (2016) 460–467.

[13] X. Wang, L. Li, J. Yang, J. Li, CO_2/CH_4 and CH_4/N_2 separation on isomeric metal organic frameworks, *Chin. J. Chem. Eng.* 24 (2016) 1687–1694.

[14] H. Xiang, X. Fan, F.R. Siperstein, Understanding ethane/ethylene adsorption selectivity in ethane-selective microporous materials, *Sep. Purif. Technol.* 241 (2020) 116635.

[15] H. Xiang, J.H. Carter, C.C. Tang, C.A. Murray, S. Yang, X. Fan, F.R. Siperstein, C_2H_4 and C_2H_6 adsorption-induced structural variation of pillared-layer CPL-2 MOF: A combined experimental and Monte Carlo simulation study, *Chem. Eng. Sci.* 218 (2020) 115566.

[16] L. Li, R.-B. Lin, R. Krishna, X. Wang, B. Li, H. Wu, J. Li, W. Zhou, B. Chen, Flexible–robust metal–organic framework for efficient removal of propyne from propylene, *J. Am. Chem. Soc.* 139 (2017) 7733–7736.

[17] L. Yang, X. Cui, Q. Yang, S. Qian, H. Wu, Z. Bao, Z. Zhang, Q. Ren, W. Zhou, B. Chen, H. Xing, A single-molecule propyne trap: Highly efficient removal of propyne from propylene with anion-pillared ultramicroporous materials, *Adv. Mater.* 30 (2018) 1705374.

[18] H.-M. Wen, L. Li, R.-B. Lin, B. Li, B. Hu, W. Zhou, J. Hu, B. Chen, Fine-tuning of nano-traps in a stable metal–organic framework for highly efficient removal of propyne from propylene, *J. Mater. Chem. A* 6 (2018) 6931–6937.

[19] L. Yang, X. Cui, Z. Zhang, Q. Yang, Z. Bao, Q. Ren, H. Xing, An asymmetric anion-pillared metal-organic framework as a multisite adsorbent enables simultaneous removal of propyne and propadiene from propylene, *Angew. Chem. Int. Ed.* 57 (2018) 13145–13149.

[20] Y.-L. Peng, C. He, T. Pham, T. Wang, P. Li, R. Krishna, K.A. Forrest, A. Hogan, S. Suepaul, B. Space, M. Fang, Y. Chen, M.J. Zaworotko, J. Li, L. Li, Z. Zhang, P. Cheng, B. Chen, Robust microporous metal-organic frameworks for highly efficient and simultaneous removal of propyne and propadiene from propylene, *Angew. Chem. Int. Ed.* 58 (2019) 10209–10214.

[21] V. Van Speybroeck, K. Hemelsoet, L. Joos, M. Waroquier, R.G. Bell, C.R.A. Catlow, Advances in theory and their application within the field of zeolite chemistry, *Chem. Soc. Rev.* 44 (2015) 7044–7111.

[22] J. Li, A. Corma, J. Yu, Synthesis of new zeolite structures, *Chem. Soc. Rev.* 44 (2015) 7112–7127.

[23] Z. Yan, S. Tang, X. Zhou, L. Yang, X. Xiao, H. Chen, Y. Qin, W. Sun, All-silica zeolites screening for capture of toxic gases from molecular simulation, *Chin. J. Chem. Eng.* 27 (2019) 174–181.

[24] S. Aguado, G. Bergeret, C. Daniel, D. Farrusseng, Absolute molecular sieve separation of ethylene/ethane mixtures with silver zeolite A, *J. Am. Chem. Soc.* 134 (2012) 14635–14637.

[25] P.J. Bereciartua, Á. Cantín, A. Corma, J.L. Jordá, M. Palomino, F. Rey, S. Valencia, E.W. Corcoran, P. Kortunov, P.I. Ravikovitch, A. Burton, C. Yoon, Y. Wang, C. Paur, J. Guzman, A.R. Bishop, G.L. Casty, Control of zeolite framework flexibility and pore topology for separation of ethane and ethylene, *Science* 358 (2017) 1068–1071.

[26] V.M. Georgieva, E.L. Bruce, M.C. Verbraeken, A.R. Scott, W.J. Casteel, S. Brandani, P.A. Wright, Triggered gate opening and breathing effects during selective CO_2 adsorption by merlinoite zeolite, *J. Am. Chem. Soc.* 141 (2019) 12744–12759.

[27] J. Shang, G. Li, R. Singh, Q. Gu, K.M. Nairn, T.J. Bastow, N. Medhekar, C.M. Doherty, A.J. Hill, J.Z. Liu, P.A. Webley, Discriminative separation of gases by a "molecular trapdoor" mechanism in chabazite zeolites, *J. Am. Chem. Soc.* 134 (2012) 19246–19253.

[28] B. Majumdar, S.J. Bhadra, R.P. Marathe, S. Farooq, Adsorption and diffusion of methane and nitrogen in barium exchanged ETS-4, *Ind. Eng. Chem. Res.* 50 (2011) 3021–3034.

[29] C.C.H. Lin, J.A. Sawada, L. Wu, T. Haastrup, S.M. Kuznicki, Anion-controlled pore size of titanium silicate molecular sieves, *J. Am. Chem. Soc.* 131 (2009) 609–614.

[30] C.A. Grande, J. Gascon, F. Kapteijn, A.E. Rodrigues, Propane/propylene separation with Li-exchanged zeolite 13X, *Chem. Eng. J.* 160 (2010) 207–214.

[31] S.M. Kuznicki, V.A. Bell, S. Nair, H.W. Hillhouse, R.M. Jacubinas, C.M. Braunbarth, B.H. Toby, M. Tsapatsis, A titanosilicate molecular sieve with adjustable pores for size-selective adsorption of molecules, *Nature* 412 (2001) 720–724.

[32] M.R. Hudson, W.L. Queen, J.A. Mason, D.W. Fickel, R.F. Lobo, C.M. Brown, Unconventional, highly selective CO_2 adsorption in zeolite SSZ-13, *J. Am. Chem. Soc.* 134 (2012) 1970–1973.

[33] M. Mofarahi, S.M. Salehi, Pure and binary adsorption isotherms of ethylene and ethane on zeolite 5A, *Adsorption* 19 (2013) 101–110.

[34] R. Seabra, V.F.D. Martins, A.M. Ribeiro, A.E. Rodrigues, A.P. Ferreira, Ethylene/ethane separation by gas-phase SMB in binderfree zeolite 13X monoliths, *Chem. Eng. Sci.* 229 (2021) 116006.

[35] Y.-X. Li, J.-X. Shen, S.-S. Peng, J.-K. Zhang, J. Wu, X.-Q. Liu, L.-B. Sun, Enhancing oxidation resistance of Cu(I) by tailoring microenvironment in zeolites for efficient adsorptive desulfurization, *Nat. Commun.* 11 (2020) 3206.

[36] H. Shang, Y. Li, J. Liu, X. Tang, J. Yang, J. Li, CH_4/N_2 separation on methane molecules grade diameter channel molecular sieves with a CHA-type structure, *Chin. J. Chem. Eng.* 27 (2019) 1044–1049.

[37] Y. Chai, X. Han, W. Li, S. Liu, S. Yao, C. Wang, W. Shi, I. Da-Silva, P. Manuel, Y. Cheng, L.D. Daemen, A.J. Ramirez-Cuesta, C.C. Tang, L. Jiang, S. Yang, N. Guan, L. Li, Control of zeolite pore interior for chemoselective alkyne/olefin separations, *Science* 368 (2020) 1002–1006.

[38] A. Anson, Y. Wang, C.C.H. Lin, T.M. Kuznicki, S.M. Kuznicki, Adsorption of ethane and ethylene on modified ETS-10, *Chem. Eng. Sci.* 63 (2008) 4171–4175.

[39] T.-H. Bae, M.R. Hudson, J.A. Mason, W.L. Queen, J.J. Dutton, K. Sumida, K.J. Micklash, S.S. Kaye, C.M. Brown, J.R. Long, Evaluation of cation-exchanged zeolite adsorbents for post-combustion carbon dioxide capture, *Energy Environ. Sci.* 6 (2013) 128–138.

[40] F.E. Epiepang, X. Yang, J. Li, Y. Wei, Y. Liu, R.T. Yang, Air separation sorbents: Mixed-cation zeolites with minimum lithium and silver, *Chem. Eng. Sci.* 198 (2019) 43–51.

[41] Y. Liu, Y. Wu, W. Liang, J. Peng, Z. Li, H. Wang, M.J. Janik, J. Xiao, Bimetallic ions regulate pore size and chemistry of zeolites for selective adsorption of ethylene from ethane, *Chem. Eng. Sci.* 220 (2020) 115636.

Supporting Information

Ultrafine tuning of the pore size in zeolite A for efficient propyne removal from propylene

Chaohui He,[1] Rajamani Krishna,[2] Yang Chen,[1] Jiangfeng Yang,[1] Jinping Li,[1] and Libo Li,[1,3]*

[1]*College of Chemistry and Chemical Engineering, Shanxi Key Laboratory of Gas Energy Efficient and Clean Utilization, Taiyuan University of Technology, Taiyuan, 030024, Shanxi, P. R. China.*

[2]*Van't Hoff Institute for Molecular Sciences, University of Amsterdam, Science Park 904, 1098 XH Amsterdam, The Netherlands.*

[3]*Key Laboratory of Coal Science and Technology, Taiyuan University of Technology, Taiyuan 030024, Shanxi, P. R. China.*

Corresponding author E-mail: lilibo908@hotmail.com

Adsorption heat

The C_3H_4 and C_3H_6 adsorption heat of the zeolites materials, Q_{st}, are defined as:

$$Q_{st} = RT^2\left(\frac{\partial \ln p}{\partial T}\right)_q \quad (1)$$

These values were determined using the pure component isotherm fits using the Virial equation (Figure S3). The adsorption heat of C_3H_4 and C_3H_6 for the selected zeolites are determined by the adsorption data measured from 0-1 bar at 273 and 298 K.

Fitting of pure component isotherms and IAST calculation

To calculate the C_3H_4/C_3H_6 (1/99) adsorption selectivity for 5A, 5A(xNa^+), 5A(yNa^+), and 5A(zNa^+) at 298 K, pure component isotherms of these ion-exchanged zeolites are fitted with Dual-site Langmuir model.

$$q = q_{A,sat}\frac{b_A p}{1 + b_A p} + q_{B,sat}\frac{b_B p}{1 + b_B p}; \quad (2)$$

The fitting parameters and fitting curves for C_3H_4 and C_3H_6 are provided in Table S2-S5 and Figure S5. The fits are of good accuracy for both guest molecules.

In order to compare the C_3H_4/C_3H_6 separation potential of these ion-exchanged zeolites, IAST calculations of mixture adsorption were performed. For separation of a binary mixture of components A and B, the adsorption selectivity is defined by

$$S_{ads} = \frac{q_A/q_B}{y_A/y_B} \quad (3)$$

where the q_A, and q_B represent the molar loadings within the MOF that is in equilibrium with a bulk fluid mixture with mole fractions y_A, and $y_B = 1 - y_A$. The IAST calculations of C_3H_4/C_3H_6 adsorption selectivites taking the mole fractions $y_A = 0.01$ and $y_B = 1 - y_A = 0.99$ for a total pressure of 100 kPa and 298 K.

Pore size distribution and surface area calculation

The pore diameter of some ion-exchanged zeolites are too small to be measured or analyzed using a N_2-sorption at 77 K (Figure S3). So the surfaces of 5A, 5A(xNa^+),

5A(yNa$^+$), and 5A(zNa$^+$) are measured and analyzed using a CO_2 sorption isotherm at 273 K. The microporous surface area and pore size distribution are calculated using the Dubinin-Radushkevitch (D-R) equation[1,2]:

$$\log(V) = \log(V_0) - \frac{B \times T^2}{\beta}(log\frac{P_0}{P})^2 \qquad (6)$$

where V was volume adsorbed at equilibrium pressure; V_0 was the micropore capacity; P_0 was saturation vapor pressure of gas at temperature T; P was equilibrium pressure; B was a constant, β was the affinity coefficient of analysis gas relative to P_0 gas (for this application β is taken to be 1); T was the analysis temperature.

Breakthrough experiments

The breakthrough curves of the selected zeolites were performed on a homemade apparatus[3] for C_3H_4/C_3H_6 (1/99 and 0.1/99.9, v/v) mixtures at a flow rate of 2 mL/min (298 K, 1.01 bar). Activated 5A(yNa$^+$) particles (4.46 g) with diameters from 220 to 300 μm were packed into ϕ 9 × 150 mm stainless steel column. The fixed-bed column was placed in a temperature controlled environment, maintained at 298 K. The flow rates of the gases mixtures were regulated by mass flow controllers, and the effluent gas stream from the column is monitored by a gas chromatography (TCD-Thermal Conductivity Detector, detection limit 0.1 ppm). Prior to each breakthrough experiment, we activated the samples by flushing the adsorption bed with helium (100 mL/min) for 30 min at 473 K.

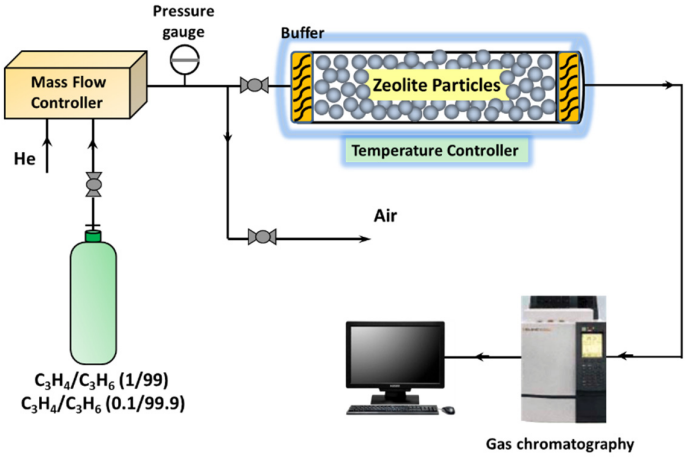

Scheme 1. Breakthrough separation apparatus

The C_3H_6 productivity (q) is defined by the capture amount of C_3H_6, conveniently expressed in the units of mol L^{-1} of adsorbent, which is calculated by integration of the breakthrough curves f(t) during a period from t_1 to t_2 where the C_3H_6 purity is higher than or equal to a threshold value:

$$q = \frac{C_i(C_3H_6)}{C_i(C_3H_6)+C_i(C_3H_4)} \times \left(\int_{t1}^{t2} f(t)dt\right)$$

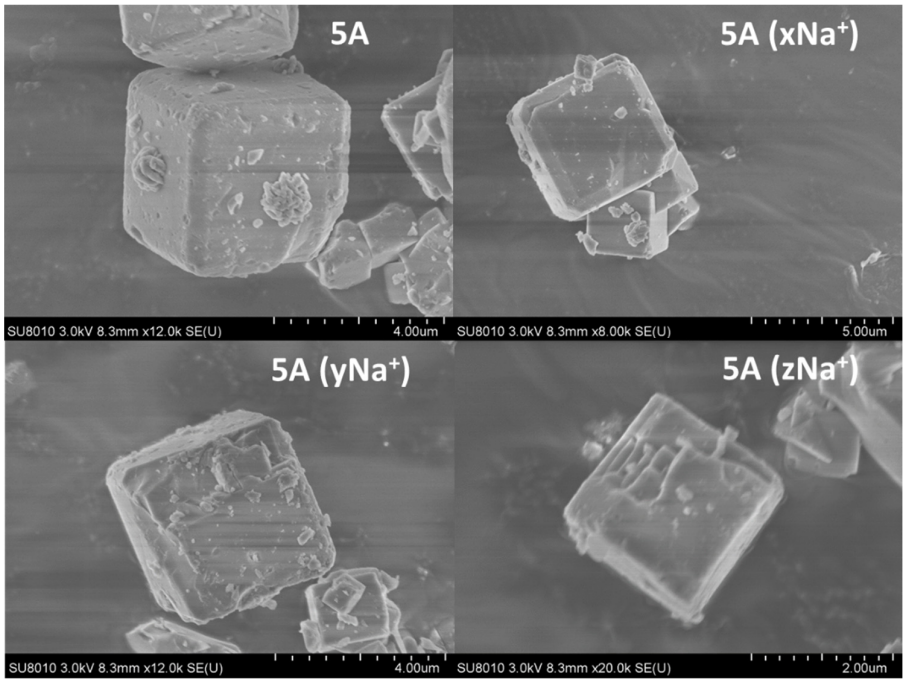

Figure S1. SEM images of 5A, 5A(xNa^+), 5A(yNa^+), and 5A(zNa^+) samples.

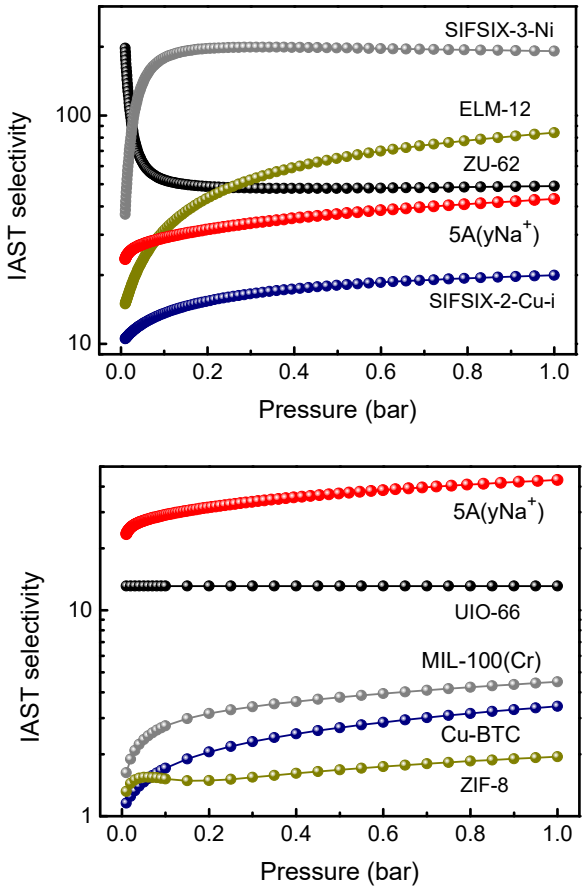

Figure S2. IAST selectivity of C_3H_4/C_3H_6 (1/99) on 5A(yNa^+) versus some MOF materials at 298 K[4].

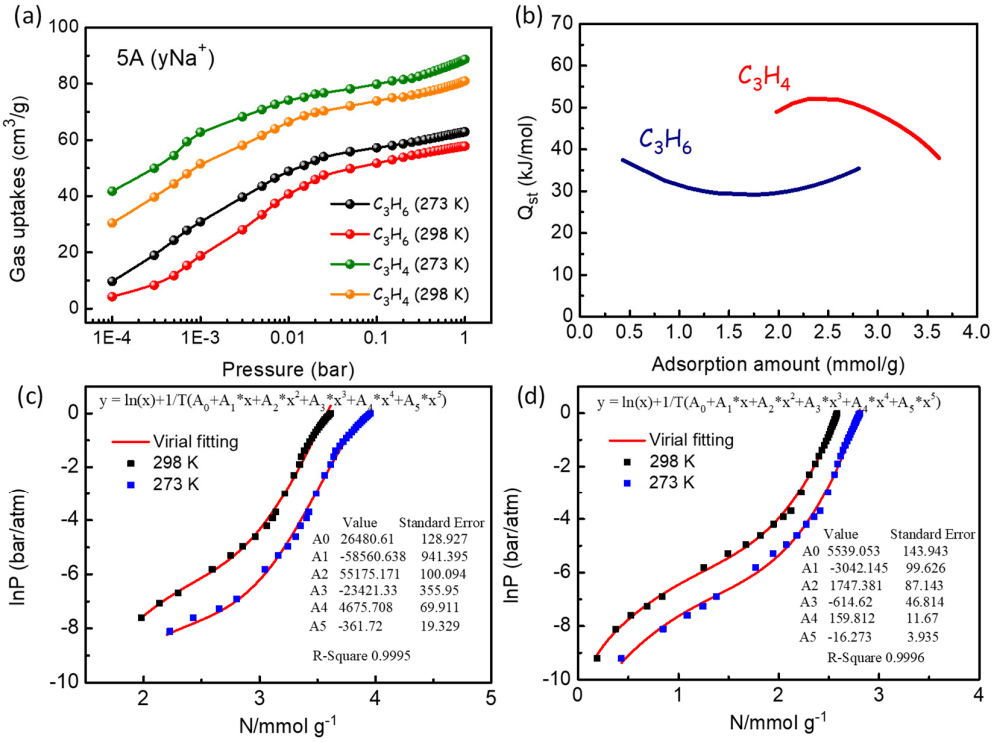

Figure S3. (a) C_3H_4 and C_3H_6 adsorption isotherms of 5A(yNa^+) at 273 and 298 K. (b) Adsorption heat and Virial fitting of (c) C_3H_4 and (d) C_3H_6 adsorption isotherms for 5A(yNa^+).

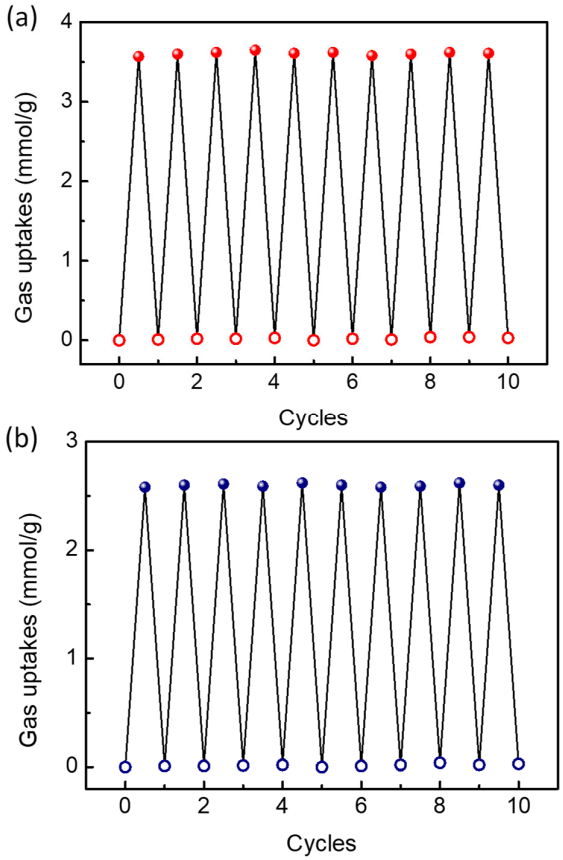

Figure S4. (a) C_3H_4 and (b) C_3H_6 adsorption cycles of 5A(yNa^+), indicating that 5A(yNa^+) maintained the C_3H_4 and C_3H_6 adsorption amount over at least 10 times. The adsorbent could totally regenerated in 5 minutes under vacuum.

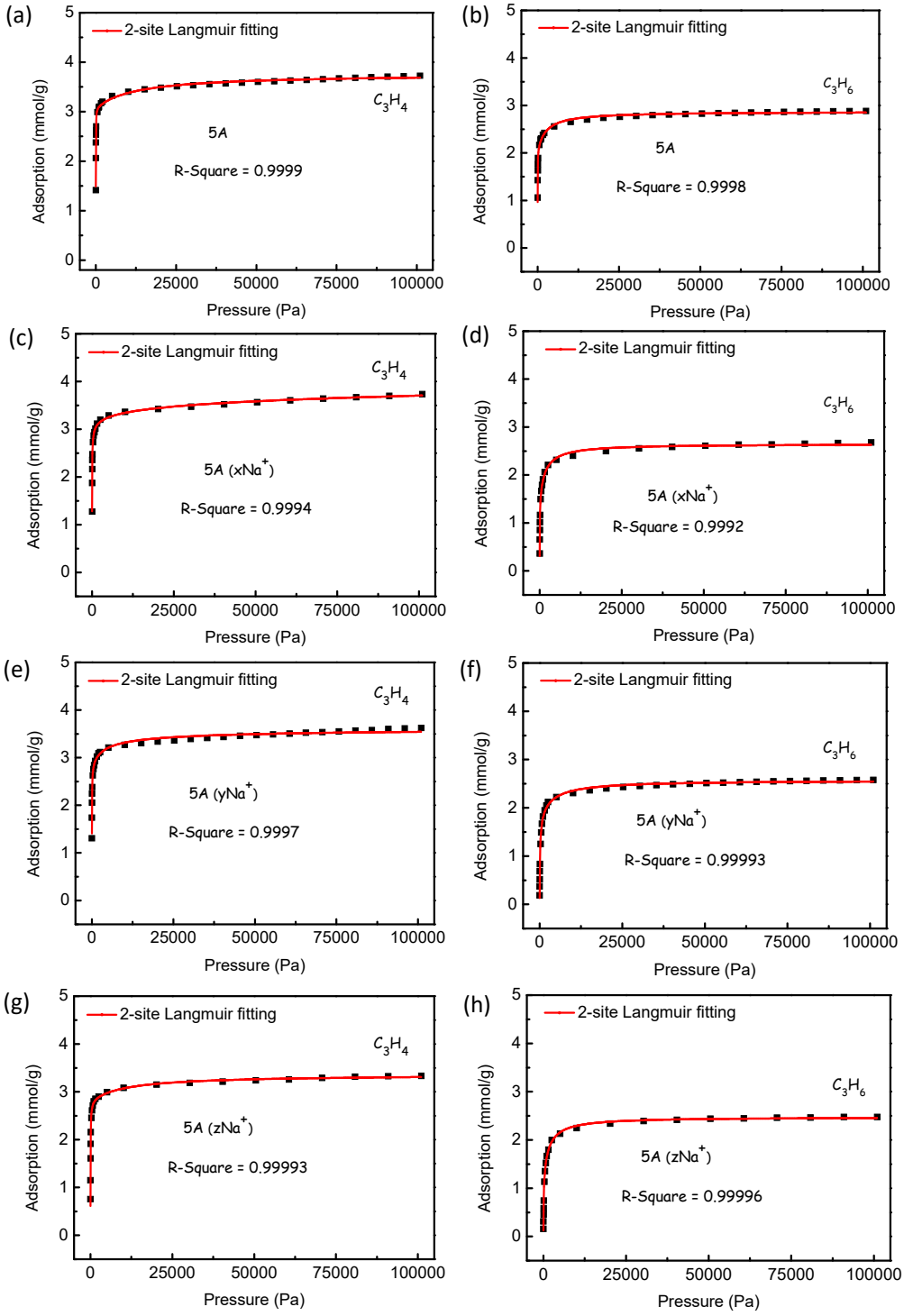

Figure S5. C_3H_4 and C_3H_6 adsorption isotherms of the ion-exchanged zeolites with dual-site Langmuir model fits.

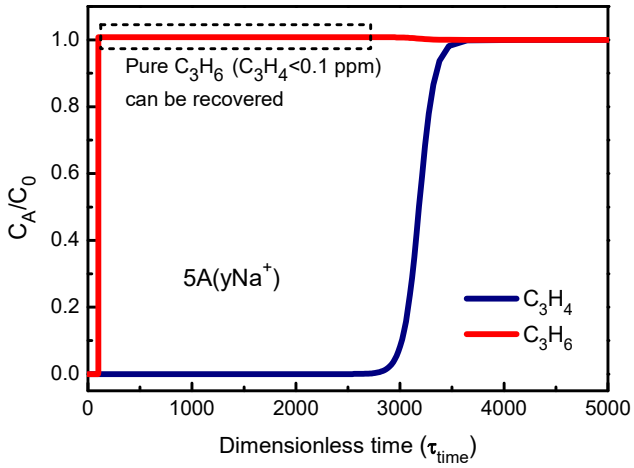

Figure S6. Transient breakthrough simulations of C_3H_4/C_3H_6 (1/99, v/v) mixture on 5A(yNa$^+$) at 298 K.

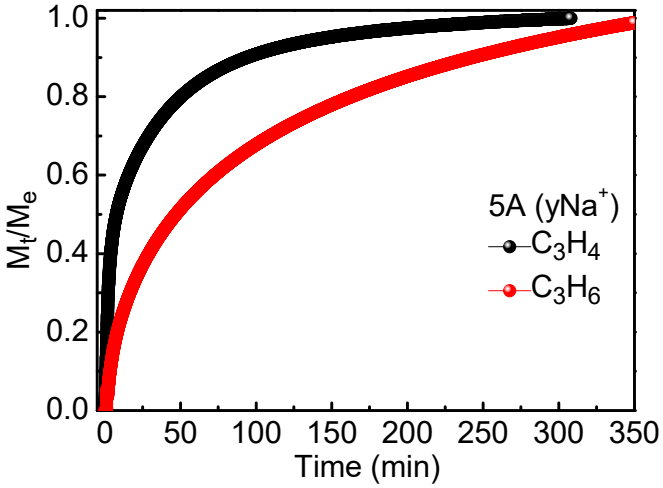

Figure S7. Kinetic adsorption profiles of C_3H_4 and C_3H_6 for 5A (yNa$^+$) at 298 K.

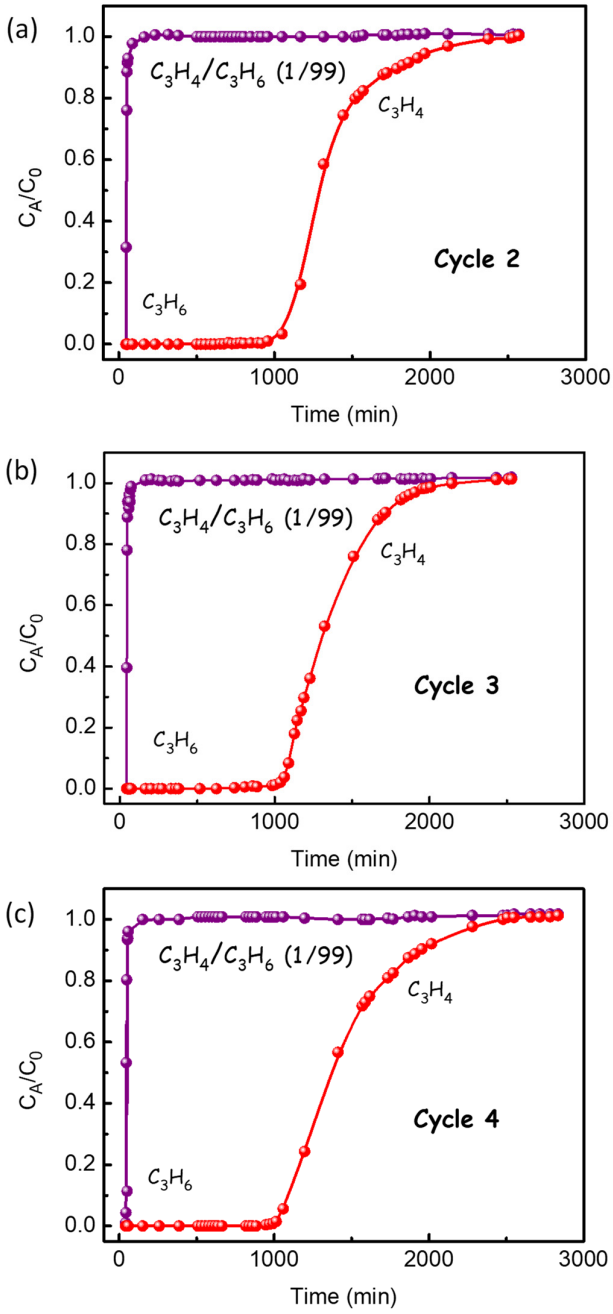

Figure S8. Cyclic breakthrough experiments for C_3H_4/C_3H_6 (1/99, v/v) separation on 5A(yNa^+) at 298 K, indicating that this material maintained the separation performance over at least 4 times.

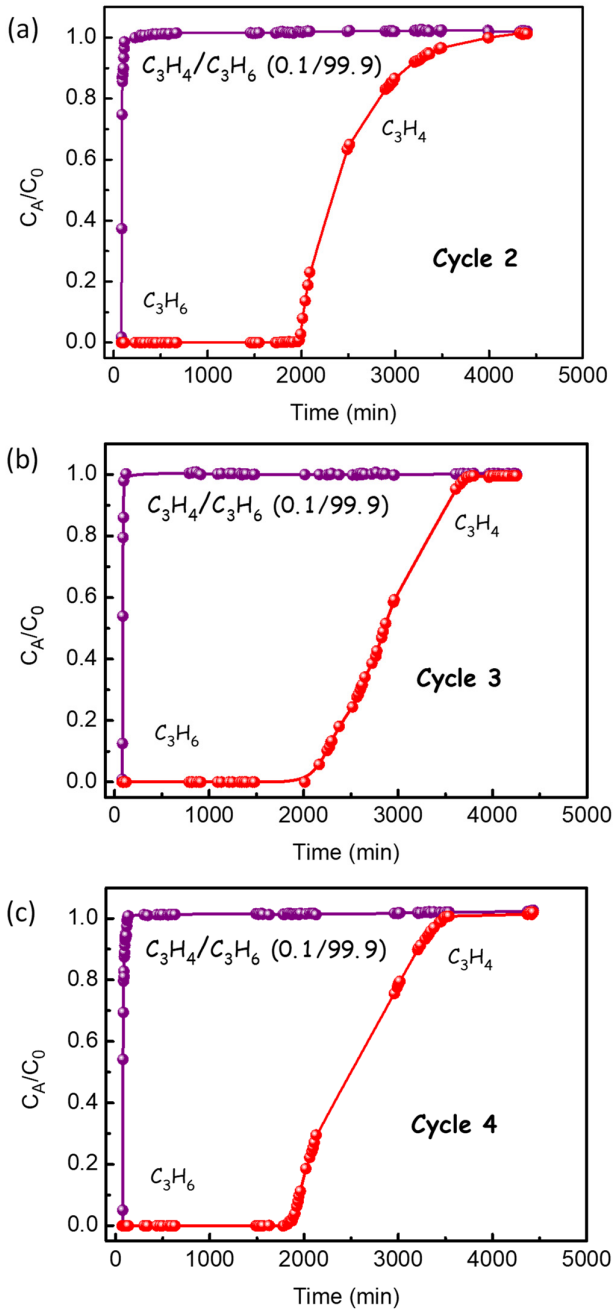

Figure S9 Cyclic breakthrough experiments for C_3H_4/C_3H_6 (0.1/99.9, v/v) separation on 5A(yNa^+) at 298 K, indicating that this material maintained the separation performance over at least 4 times.

Table S1. Chemical composition and BET surface areas (based on the CO_2 adsorption isotherms) of the samples.

	Ca (mmol/g)	Na (mmol/g)	Sample density (kg L^{-1})	Surface area (m^2/g)
5A	2.21	3.33	0.94	508
5A (xNa^+)	1.26	4.32	1.14	538
5A (yNa^+)	0.74	5.41	1.16	503
5A (zNa^+)	0.53	5.43	1.05	435

Table S2. 2-site Langmuir fitting parameters for C_3H_4 and C_3H_6 in 5A.

	Site A		**Site B**	
	$q_{A,sat}$ mmol g^{-1}	b_A Pa^{-1}	$q_{B,sat}$ mmol g^{-1}	b_B Pa^{-1}
C_3H_4	3.1	9.00E-02	0.7	6.14E-05
C_3H_6	2	1.01E-01	0.9	4.10E-04

Table S3. 2-site Langmuir fitting parameters for C_3H_4 and C_3H_6 in 5A (xNa^+).

	Site A		**Site B**	
	$q_{A,sat}$ mmol g^{-1}	b_A Pa^{-1}	$q_{B,sat}$ mmol g^{-1}	b_B Pa^{-1}
C_3H_4	2.7	8.44E-02	0.9	5.44E-04
C_3H_6	1.4	3.07E-02	1.25	7.54E-04

Table S4. 2-site Langmuir fitting parameters for C_3H_4 and C_3H_6 in 5A (yNa^+).

	Site A		Site B	
	$q_{A,sat}$ mmol g^{-1}	b_A Pa^{-1}	$q_{B,sat}$ mmol g^{-1}	b_B Pa^{-1}
C_3H_4	2.5	9.71E-02	1	7.30E-04
C_3H_6	1	1.77E-02	1.5	1.29E-03

Table S5. 2-site Langmuir fitting parameters for C_3H_4 and C_3H_6 in 5A (zNa^+).

	Site A		Site B	
	$q_{A,sat}$ mmol g^{-1}	b_A Pa^{-1}	$q_{B,sat}$ mmol g^{-1}	b_B Pa^{-1}
C_3H_4	2.8	2.91E-02	0.55	1.11E-04
C_3H_6	1.1	1.29E-02	1.35	8.54E-04

Table S6. Breakthrough calculations for separation of C_3H_4/C_3H_6 (1/99) mixture at 298 K.

	Separation potential ΔQ (mol/L)	Breakthrough productivity of C_3H_6 (mol/L)
UTSA-200	404.5	367.2
SIFSIX-3-Ni	210.1	182.2
5A(yNa^+)	**90.5**	**71.7**
SIFSIX-2-Cu-i	64.8	47.7
Cu-BTC	18.7	/
MIL-100(Cr)	15.8	9.9
UIO-66	47.4	31.8
ZIF-8	3.6	1.6

Table S7. Summary of the equilibrium uptakes and C_3H_4/C_3H_6 selectivity in 5A (yNa^+) and some previous reported MOFs.

Adsorbents	Temperature (K)	C_3H_4 uptake (mmol/g)	C_3H_6 uptake (mmol/g)	C_3H_4/C_3H_6 selectivity
5A (yNa^+)	298	3.62	2.58	43
SIFSIX-3-Ni	298	2.85	2.72	76
ELM-12	298	2.77	1.43	83
ZU-62	298	3.64	2.67	48
SIFSIX-2-Cu-i	298	3.77	2.19	30
UiO-66	298	10.23	3.33	13.1
MIL-100(Cr)	298	14.51	6.25	4.4
Cu-BTC	298	10.47	8.33	3.4
ZIF-8	293	6.27	4.07	1.9

References

[1] M.M. Dubinin, Microporous structures and absorption properties of carbonaceous adsorbents, *Carbon* 21 (1983) 359-366.

[2] J. Yang, Q. Zhao, H. Xu, L. Li, J. Dong, J. Li, Adsorption of CO_2, CH_4, and N_2 on Gas Diameter Grade Ion-Exchange Small Pore Zeolites, *J. Chem. Eng. Data* 57 (2012) 3701-3709.

[3] L. Li, R.-B. Lin, R. Krishna, X. Wang, B. Li, H. Wu, J. Li, W. Zhou, B. Chen, Flexible–robust metal–organic framework for efficient removal of propyne from propylene, *J. Am. Chem. Soc.* 139 (2017) 7733-7736.

[4] L. Li, H.-M. Wen, C. He, R.-B. Lin, R. Krishna, H. Wu, W. Zhou, J. Li, B. Li, B. Chen, A Metal–Organic Framework with Suitable Pore Size and Specific Functional Sites for the Removal of Trace Propyne from Propylene, *Angew. Chem. Int. Ed.* 57 (2018) 15183-15188.